

# STRONG GEOMETRY: KNOTS

BAPTISTE GROS<sup>1</sup> AND JORGE L. RAMÍREZ ALFONSÍN

ABSTRACT. In this paper, we introduce the notion of *strong geometry*, a structure composed by both the chirotope of the oriented matroid associated to a set of points  $X$  in the  $d$ -dimensional space and a new chirotope induced by the hyperplanes spanned by  $X$ . With this on hand, we answer positively a strong geometry version of a question due to M. Las Vergnas about reconstructing polygonal knots via oriented matroids.

## 1. INTRODUCTION

Many problems in discrete and convex geometry are based on finite sets of points in the Euclidean space. The combinatorial properties of the underlying point set, rather than its metric properties, are enough to solve a large number of such problems. Indeed, oriented matroids (initially known as *combinatorial geometries*) are natural combinatorial objects to study questions concerning the relatively positions of a set of points in the space (not taking into account distances) [1]. For instance, the intersection properties of the line segments spanned by a set of points in the plane turn out to be of great importance. It is well-known that this intersecting properties are exactly reflected by the *order type* of a point set, introduced in [4]. This geometric condition is well codified combinatorially by the corresponding oriented matroid in terms of the notion of *chirotopes* (or its signed circuits). Although oriented matroids give information about such intersections, it does not tell anything about the *relative positions* of such intersections with respect to the set of spanned lines. The knowledge of the latter might play a key role in the study of certain geometric problems. For instance, Figure 1 illustrates two hexagons having the same affine oriented matroid induced by their vertices (they both have the same set of circuits or equivalently set of minimal Radon partitions). However, in the hexagon on the left the lines joining opposite vertices intersect at point  $p$  while they do not in the right one.

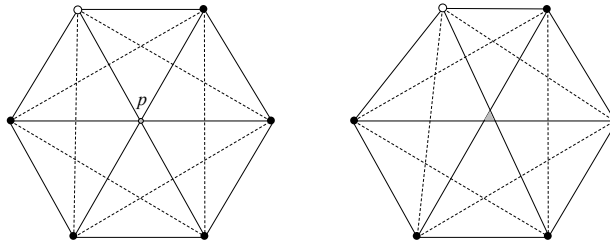


FIGURE 1. (Left) A regular hexagon where point  $p$  (in gray) is the intersection of lines joining opposite vertices. (Right) The same regular hexagon in which a vertex (in white) has been slightly moved to the right. The lines joining opposite vertices form a triangle (in gray).

2010 *Mathematics Subject Classification.* 52C140, 57K10.

*Key words and phrases.* Oriented Matroid, Chirotope, Knot.

<sup>1</sup> Partially supported by grant PRIM80-CNRS.

It turns out that  $p$  is a *0-transversal* to the convex hull of the 4-sets (that is,  $p$  intersects all 4-sets formed by the vertices). It can be easily checked that the hexagon on the right does not admit a 0-transversal. In fact, such *discrete transversal* is not necessarily an invariant of the order type, see [3].

This is a typical situation in which the knowledge of the position of the intersection of two lines, with respect with the other spanned lines, is helpful (in this case for a transversality-type problem).

In this paper, we introduce the notion of *strong geometry*. This structure is composed by not only the chirotope of the oriented matroid associated to a set of points  $X$  in  $\mathbb{R}^d$ ,  $d \geq 2$  but also by a new chirotope induced by the hyperplanes spanned by  $X$ . As we will see, in dimension 2, strong geometries encode nicely the combinatorics of the cells of the arrangement of the spanned lines.

After introducing and discussing properties of the notion of strong geometry, we shall present a first topological application in connection with geometric knots. A *knot* is an embeddings of  $S^1$  into  $\mathbb{R}^3$  up to isotopy. In order to avoid pathologies, it is common to study tame knots, in particular, *polygonal knots*, that is, closed, piecewise linear loops with no self-intersections consisting of  $n$  segments in  $\mathbb{R}^3$ . Not much is known about the interplay between the classic setting and *geometric knots*, which are polygonal knots with a fixed number of segments of variable length. Geometric knots are more rigid than smooth knots and they better suited for describing macromolecules (such as DNA) in polymer chemistry and molecular biology, but also far more resistant to investigation.

Let  $X = (x_0, \dots, x_{n-1})$  be a  $n$ -tuple of points in  $\mathbb{R}^3$  in general position. Let  $K_X$  be the polygonal knot defined by the segments  $[x_i, x_{i+1}]$  (addition  $(\text{mod } n)$ ). Michel Las Vergnas [7] has put forward the following

**Question 1.** *Let  $X = (x_0, \dots, x_{n-1})$  be a  $n$ -tuple of points in  $\mathbb{R}^3$  in general position. Is it true that  $K_X$  only depends on the affine oriented matroid induced by  $x_0, \dots, x_{n-1}$  ?*

We are able to give a positive answer to Las Vergnas' question in the case of strong geometries.

**Theorem 1.** *Let  $X = (x_0, \dots, x_{n-1})$  and  $X' = (x'_0, \dots, x'_{n-1})$  be two  $n$ -tuples of points in  $\mathbb{R}^3$  in general position. Let  $\text{SGeom}_{\text{Aff}}(X)$  and  $\text{SGeom}_{\text{Aff}}(X')$  be the strong geometries associated to  $X$  and  $X'$  respectively. If  $\text{SGeom}_{\text{Aff}}(X)$  is isomorphic to  $\text{SGeom}_{\text{Aff}}(X')$  then  $K_X$  is isotopic to  $K_{X'}$ .*

## 2. ORIENTED MATROID PRELIMINARIES

For general background in oriented matroid theory we refer the reader to the book [1]. An *oriented matroid*  $M = (E, \chi)$  of rank  $r$  is a finite set  $E = \{1, \dots, n\}$  together with a function  $\chi : E^r \rightarrow \{-1, 0, 1\}$ , called *chirotope* verifying the following conditions

(CH0)  $\chi$  is not always zero,

(CH1)  $\chi$  is *alternating*, that is, for all  $\{i_1, \dots, i_r\} \subset E$  and all  $\sigma \in \mathfrak{S}_r$ , we have

$$\chi(i_{\sigma(1)}, \dots, i_{\sigma(r)}) = \epsilon(\sigma)\chi(i_1, \dots, i_r),$$

(CH3) for all  $\{i_1, \dots, i_r\}, \{j_1, \dots, j_r\} \subset E$  such that

$$\chi(j_k, i_2, \dots, i_r)\chi(j_1, \dots, j_{k-1}, i_1, j_{k+1}, \dots, j_r) \geq 0$$

for all  $k$ , then

$$\chi(i_1, \dots, i_r)\chi(j_1, \dots, j_r) \geq 0.$$

Let  $1 \leq d \leq n$  be integers. To each configuration of vectors  $X = (\mathbf{x}_1, \dots, \mathbf{x}_n) \in (\mathbb{R}^d)^n$ , we may associate an oriented matroid  $M = (E, \chi)$  of rank  $d$  by taking

$$\chi(i_1, \dots, i_d) = \Delta(\mathbf{x}_{i_1}, \dots, \mathbf{x}_{i_d}) \in \{-1, 0, 1\}.$$

where  $\Delta = \text{sign} \circ \det$ , that is, the sign of the determinant.

$M$  is called *linear* or *vectorial* and it is denoted by  $M_{\text{Lin}}(X)$ .

We may also associate an oriented matroid  $M = (E, \chi)$  of rank  $r(M) = d + 1$  to a configuration of points  $X = \{x_1, \dots, x_n\}$  in the affine space  $\mathbb{R}^d$  by taking

$$\chi(i_1, \dots, i_d) = \Delta \begin{pmatrix} 1 & \cdots & 1 \\ x_{i_1} & \cdots & x_{i_d} \end{pmatrix}.$$

$M$  is called *affine* and it is denoted by  $M_{\text{Aff}}(X)$ .

We notice that we can pass from affine to linear matroids by considering the inclusion

$$\text{in} : \mathbb{R}^d \simeq \{1\} \times \mathbb{R}^d \subset \mathbb{R}^{d+1}.$$

We may thus write  $\mathbf{x}$  instead of  $x$  to distinguish vectors from points. From now on, when we refer  $\mathbb{R}^d$  as *affine space*, we mean that it is included in  $\mathbb{R}^{d+1}$  as  $\{1\} \times \mathbb{R}^d$ .

Let us recall that a set  $P = \{p_1, \dots, p_n\}$  of  $n \geq d + 2$  points in  $\mathbb{R}^d$  always admits a *Radon partition*, that is, a partition  $P = A \sqcup B$  such that  $\text{conv}(\{p_i \mid p_i \in A\}) \cap \text{conv}(\{p_i \mid p_i \in B\}) \neq \emptyset$ . It is known that a circuit  $C = C^+ \cup C^-$  of an affine oriented matroid associated to a set of points  $\{y_1, \dots, y_n\}$  corresponds to a minimal Radon partition, that is,  $\text{conv}(\{y_i \mid i \in C^+\}) \cap \text{conv}(\{y_i \mid i \in C^-\}) \neq \emptyset$ . We have that a Radon partition of  $\{x_1, \dots, x_{d+2}\}$  admits both  $x_{d+1}$  and  $x_{d+2}$  in either  $A$  or  $B$  if and only if  $\chi(x_1, \dots, x_d, x_{d+1}) = -\chi(x_1, \dots, x_d, x_{d+2})$ . Therefore, Radon's partitions can be recovered from the chirotope.

### 3. STRONG GEOMETRIES

We shall first introduce and discuss the notion of strong geometries when  $d = 2$  for a better comprehension of this notion. We then treat strong geometries for general  $d \geq 3$ .

**3.1. Planar case.** Let  $X$  be a set of points in  $\mathbb{R}^2$ . As mentioned above, strong geometries intend to capture more geometric information than ordinary oriented matroids, specifically, the relative positions of triples of lines generated by points in  $X$ . Instead of consider the rank 3 affine oriented matroid associated to  $X$ , we may thought the affine geometry of dimension 2 as a linear geometry in dimension 3. This setting happen to be more convenient, for our propose. Since we are only interested in computing signs of multi-linear expressions then we do not worry about the norm of the vectors in  $\mathbb{R}^3$ . The points in  $X$  will be associated to vectors living in  $\mathbb{R}^3/(\mathbb{R}_+)$  which in turn will be thought of as  $\mathbb{S}^d \cup \{0\}$  for a nicer visualisation.

Let  $x$  and  $y$  be two points in the affine space  $\mathbb{R}^2 \subset \mathbb{R}^3$ . Let  $l_{x,y}$  be the equator arising from the intersection of the (oriented) plane  $h_{x,y}$  spanned by  $x$  and  $y$  and  $\mathbb{S}^3$ . Let  $\mathbf{x}$  and  $\mathbf{y}$  be the vectors on  $l_{x,y}$  arising from intersection of  $\mathbb{S}^2$  and the line segments  $[0, x]$  and  $[0, y]$  respectively. Equator  $l_{x,y}$  is oriented from  $\mathbf{x}$  to  $\mathbf{y}$  if  $(\mathbf{x}, \mathbf{y})$  is a positive basis, see Figure 2.

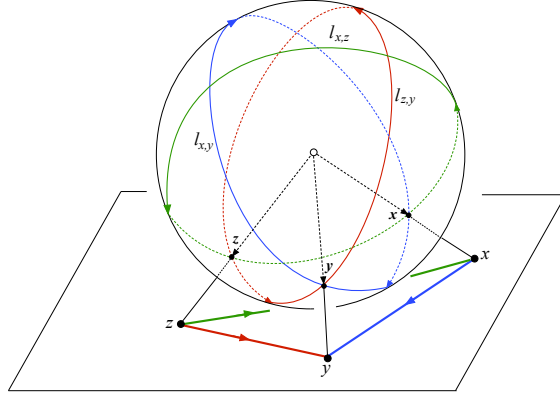


FIGURE 2. Unit vectors associated to points in the plane.

The hyperplane  $h_{x,y}$  is parametrized by the normal positive (norm 1) vector given by the product  $\mathbf{x} \times \mathbf{y}$ . We may write  $\wedge$  the image of  $\times$  in  $\mathbb{R}^3/(\mathbb{R}_+)$ . In the degenerate case, we consider the 0 vector to be the equator between two antipodal (equal) points, see Figure 3.

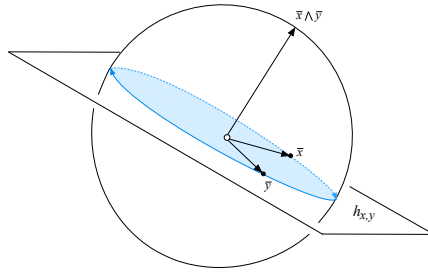


FIGURE 3

**Remark 1.** Let  $l$  be an oriented equator of  $\mathbb{S}^3$  with positive normal vector  $v_l$  and let  $l^+$  (resp.  $l^-$ ) be the positive (resp. negative) half-sphere delimited by  $l$ . Let  $\mathbf{p}$  be a vector in  $\mathbb{S}^2$ . Then,

$$\mathbf{p} \in \begin{cases} l^+ & \text{if } \langle \mathbf{v}_l, \mathbf{p} \rangle > 0, \\ l^- & \text{if } \langle \mathbf{v}_l, \mathbf{p} \rangle < 0, \\ l & \text{if } \langle \mathbf{v}_l, \mathbf{p} \rangle = 0. \end{cases}$$

where  $\langle \mathbf{u}, \mathbf{v} \rangle$  denotes the scalar product of vectors  $\mathbf{u}$  and  $\mathbf{v}$ .

Let  $x, y$  and  $z$  be points in the affine space. One may determine whether  $z$  is in the positive or negative half-space delimited by the oriented line from  $x$  to  $y$  by considering  $\text{sign}(\det(x, y, z))$ . In a similar manner, this can be determined by considering the vectors  $\mathbf{x}, \mathbf{y}, \mathbf{z} \in \mathbb{S}^2$ . Indeed, by Remark 1,  $\text{sign}(\langle \mathbf{x} \times \mathbf{y}, \mathbf{z} \rangle)$  determines whether  $\mathbf{z}$  is in the positive or negative half-sphere delimited by  $l_{x,y}$  oriented from  $x$  to  $y$ . The latter is simply due to the elementary property of the determinant

$$(1) \quad \text{sign}(\det(x, y, z)) = \text{sign}(\langle \mathbf{x} \times \mathbf{y}, \mathbf{z} \rangle).$$

Dealing with equators in the sphere makes things easier. In affine geometry there are numerous ways that three oriented lines may met, see Figure 4 while generic triplets of oriented equators can only be of two combinatorial types, see Figure 5.

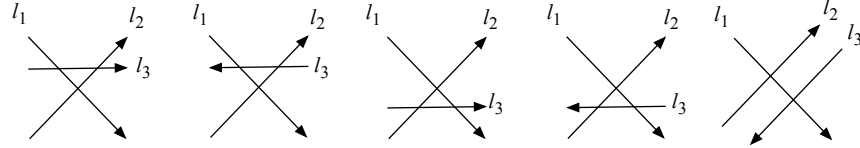


FIGURE 4. Some of the non-isotopic triplets of oriented lines.

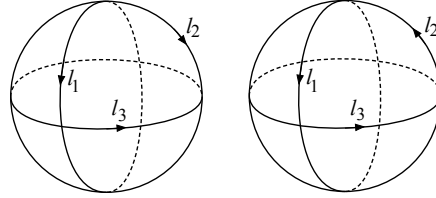


FIGURE 5. Positive and negative triplets of equators.

Let  $l_1$  and  $l_2$  be two equators and let  $\mathbf{v}_1$  and  $\mathbf{v}_2$  be the normal vectors of the corresponding hyperplanes supporting  $l_1$  and  $l_2$  respectively. If  $l_1$  and  $l_2$  are *colinear*, i.e. equal or opposite, then the sign associated to any triple  $(l_1, l_2, l_3)$  is always 0. Otherwise, they meet at two antipodal points  $p$  and  $-p$ , in this case,  $\mathbf{v}_1 \wedge \mathbf{v}_2$  is one of these points, we call it *positive intersection*, see Figure 6.

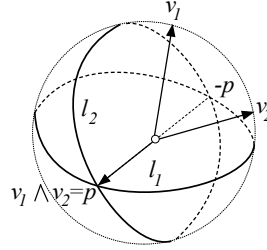


FIGURE 6

We thus have that a third equator  $l_3$  admits either  $p$  or  $-p$  on its positive half-sphere (the other in the negative half-sphere). Analogously to the dual case above (1), we define the sign associated to a triple of equators  $l_1, l_2$  and  $l_3$  as

$$(2) \quad \text{sign}(l_1, l_2, l_3) := \text{sign}(\langle \mathbf{v}_1 \times \mathbf{v}_2, \mathbf{v}_3 \rangle).$$

This leads us to define a chirotope  $\chi_\Lambda$  on the set of equators by

$$\chi_\Lambda(i, j, k) := \text{sign}(l_i, l_j, l_k).$$

We call  $\chi_\Lambda$  a *wedge* chirotope.

Note that if  $l_i = \mathbf{x}_i \wedge \mathbf{y}_i$ ,  $l_j = \mathbf{x}_j \wedge \mathbf{y}_j$  and  $l_k = \mathbf{x}_k \wedge \mathbf{y}_k$ , then we also have

$$(3) \quad \chi_\Lambda(i, j, k) = \Delta\left(\left(\mathbf{x}_i \wedge \mathbf{y}_i\right) \wedge \left(\mathbf{x}_j \wedge \mathbf{y}_j\right), \mathbf{x}_k, \mathbf{y}_k\right).$$

**3.2. General setting.** We shall generalize the wedge chirotope to higher dimensions. To this end, we use the natural generalization of the cross product to higher dimension.

Let  $d \geq 2$  and let  $X = (\mathbf{x}_1, \dots, \mathbf{x}_d)$  be a  $d$ -tuple of vectors in  $\mathbb{R}^{d+1}$  (or in  $\mathbb{S}^d$ ). If the family  $(\mathbf{x}_1, \dots, \mathbf{x}_d)$  is independent then we define  $\boldsymbol{\alpha}(X)$  to be the (norm 1)  $(d+1)$ -dimensional vector orthogonal to all  $\mathbf{x}_i$ 's (i.e., orthogonal to the hyperplane  $h(X)$  spanned by the  $\mathbf{x}_i$ 's) and such that  $\det(\mathbf{x}_1, \dots, \mathbf{x}_d, \boldsymbol{\alpha}(X)) > 0$ . We call  $\boldsymbol{\alpha}(X)$  an *hyperplane-vector*. If  $(\mathbf{x}_1, \dots, \mathbf{x}_d)$  is dependent then we set  $\boldsymbol{\alpha}(X) = \mathbf{0}$  (in this case the hyperplane vector is *degenerate*).

Let  $\mathcal{H} = \{h(I) \mid I \in [n]^d\}$ . We may also suppose that the elements in  $\mathcal{H}$  are ordered, that is, if  $h_i = h(I)$  and  $h_j = h(J)$  then  $h_i < h_j$  if  $I < J$  (in lexicographic order).

Let  $\Lambda(X)$  be the family of all hyperplane-vectors, that is,

$$\Lambda(X) = \left( \boldsymbol{\alpha}(X_I) \right)_{I \in [n]^d}$$

For short, we may write  $\Lambda(X) = \left( \boldsymbol{\alpha}(I) \right)_{I \in [n]^d}$ .

We define the *wedge oriented matroid*, denoted by  $M_{\text{Wedge}}(X)$ , as the oriented matroid  $M_{\text{Lin}}(\Lambda(X))$ , that is, the  $(d+1)$ -rank oriented matroid with base set  $[n]^d$  and with chirotope function  $\chi_\Lambda$  verifying

$$\chi_\Lambda(I_1, \dots, I_{d+1}) = \Delta(\boldsymbol{\alpha}(I_1), \dots, \boldsymbol{\alpha}(I_{d+1}))$$

for  $I_1, \dots, I_{d+1} \in [n]^d$ .

Similarly as in the 2-dimensional case (i.e., rank 3), in the same flavor as Equation (3), we have the following result which is a straight consequence of the definition of  $\boldsymbol{\alpha}$ .

**Lemma 1.** *Let  $X_1, \dots, X_d, Y$  be  $(d+1)$   $d$ -tuples of vectors in  $\mathbb{R}^d$  and let  $Y = (\mathbf{y}_1, \dots, \mathbf{y}_d)$ . Then,*

$$\begin{aligned} \Delta(\boldsymbol{\alpha}(X_1), \dots, \boldsymbol{\alpha}(X_d), \boldsymbol{\alpha}(Y)) &= \text{sign}(\langle \boldsymbol{\alpha}(\boldsymbol{\alpha}(X_1), \dots, \boldsymbol{\alpha}(X_d)), \boldsymbol{\alpha}(Y) \rangle) \\ &= \Delta(\boldsymbol{\alpha}(X_1), \dots, \boldsymbol{\alpha}(X_d), \mathbf{y}_1, \dots, \mathbf{y}_d). \end{aligned}$$

We define the *strong geometry* associated to  $X$ , denoted by  $\text{SGeom}_{\text{Lin}}(X)$ , as the structure composed by the couple  $(M_{\text{Lin}}(X), M_{\text{Wedge}}(X))$ . We may also consider the affine version  $\text{SGeom}_{\text{Aff}}(X) = (M_{\text{Aff}}(X), M_{\text{Wedge}}(\text{in}(X)))$ . Strong geometry will determine helpful complementary geometric information on the set  $X$ . Moreover, the chirotopes  $\chi$  and  $\chi_\Lambda$  are closely related as it is highlighted in the following two propositions.

**Proposition 1.** *Let  $P = \{p_a, p_b, p_c, p_x, p_y\}$  be points in the affine space  $\mathbb{R}^2 \subset \mathbb{R}^3$ . Let  $h_1, h_2$  and  $h_3$  be the planes spanned by the couples of 3-dimensional vectors  $I_1 = (\mathbf{p}_a, \mathbf{p}_b)$ ,  $I_2 = (\mathbf{p}_a, \mathbf{p}_c)$  and  $I_3 = (\mathbf{p}_x, \mathbf{p}_y)$  respectively. Recall that  $\boldsymbol{\alpha}(I_1) = \mathbf{p}_a \wedge \mathbf{p}_b$ ,  $\boldsymbol{\alpha}(I_2) = \mathbf{p}_a \wedge \mathbf{p}_c$  and  $\boldsymbol{\alpha}(I_3) = \mathbf{p}_x \wedge \mathbf{p}_y$ . Then,*

$$(4) \quad \chi_\Lambda(I_1, I_2, I_3) = \chi(a, b, c)\chi(a, x, y).$$

*Proof.* If  $\chi(a, b, c) = 0$  then the equality (4) can be easily checked. Let us thus suppose that  $\chi(a, b, c) \neq 0$ , that is,  $p_a, p_b$  and  $p_c$  are points in generic position. Since  $\mathbf{p}_a$  is in both  $l_1 = \mathbf{p}_a \wedge \mathbf{p}_b$  and  $l_2 = \mathbf{p}_a \wedge \mathbf{p}_c$ , then the positive intersection of equators  $l_1$  and  $l_2$  is either  $p_a$  if  $\chi(a, b, c) = +1$  or  $-p_a$  if  $\chi(a, b, c) = -1$  (if  $\chi(a, b, c) = 0$  then  $\mathbf{p}_a \wedge \mathbf{p}_b$  and  $\mathbf{p}_a \wedge \mathbf{p}_c$  are colinear). This is due to the fact there is only one isotopy class of positive triples of vectors.

We have that (4) can be thus stated as

$$(\mathbf{p}_a \wedge \mathbf{p}_b) \wedge (\mathbf{p}_a \wedge \mathbf{p}_c) = \chi(a, b, c) \mathbf{p}_a.$$

Combining this equality with

$$\chi_\Lambda(I_1, I_2, I_3) = \text{sign}(\langle (\mathbf{p}_a \wedge \mathbf{p}_b) \wedge (\mathbf{p}_a \wedge \mathbf{p}_c), (\mathbf{p}_x \wedge \mathbf{p}_y) \rangle)$$

the desired equality follows. □

Figure 7 gives a visual explanation of Proposition 1 in the affine setting.

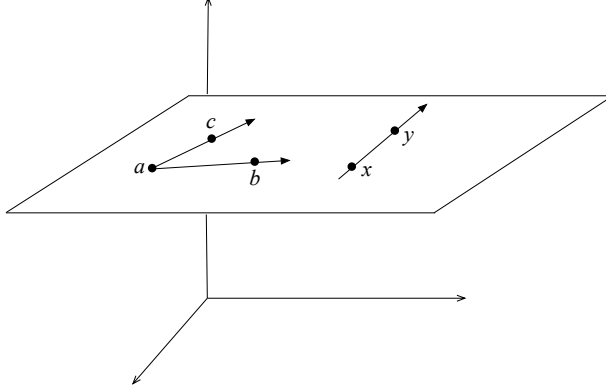


FIGURE 7

We notice that Proposition 1 implies that two  $n$ -tuples with the same strong geometry have either equal or opposite chirotopes. Let us extend Proposition 1 to affine space in  $\mathbb{R}^d$ . For, we first introduce the *witness* oriented matroid which will play a central role in the proof of our main result. Let  $\omega, x_1, \dots, x_n$  be a configuration of points in the affine space  $\mathbb{R}^d$  where the point  $\omega$ , called the *witness*, will play a special role.

The *witness* oriented matroid from  $\omega$ , denoted by  $M_{\text{Wit}_\omega}(X)$ , is the linear oriented matroid  $M_{\text{Lin}}(W_\omega(X))$  where  $W_\omega(X) = \{x_1 - \omega, \dots, x_n - \omega\}$ . Notice that  $M_{\text{Wit}_\omega}(X)$  is of rank  $d$  since the vectors  $x_i - \omega$  are considered in  $\mathbb{R}^d$  instead of vectors in  $\mathbb{R}^{d+1}$ , see Figure 8.

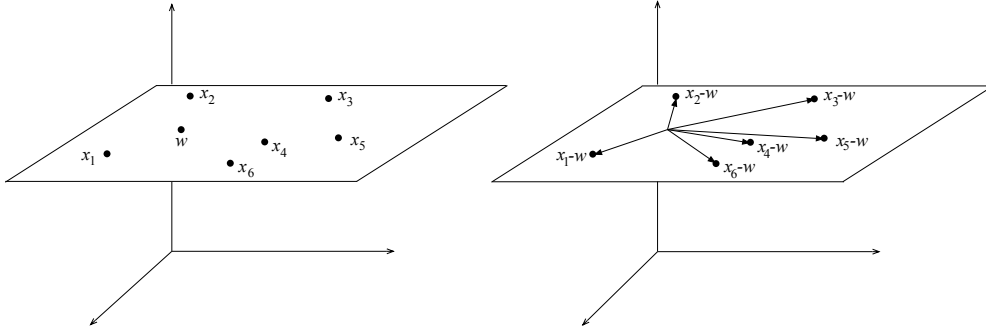


FIGURE 8. (Left) Affine oriented matroid of rank 3 associated to points  $\omega, x_1, \dots, x_6$ . (Right) Witness oriented matroid of rank 2 associated to vectors  $\mathbf{x}_1 - \omega, \dots, \mathbf{x}_6 - \omega$ .

**Proposition 2.** Let  $n \geq 1$  be an integer and let  $X = (\omega = x_0, x_1, \dots, x_n)$  be a tuple of points in  $\mathbb{R}^3$ . Let  $i_0 = 0, i_1, \dots, i_9 \in [n]^9$  and let  $I_1 = (i_0, i_1, i_2), I_2 = (i_0, i_3, i_4), I_3 = (i_0, i_5, i_6)$  and  $J = (i_7, i_8, i_9)$ . Let  $\mathbf{x}_{a_1} = (x_{i_1} - \omega) \wedge (x_{i_2} - \omega), \mathbf{x}_{a_2} = (x_{i_3} - \omega) \wedge (x_{i_4} - \omega)$  and  $\mathbf{x}_{a_3} = (x_{i_5} - \omega) \wedge (x_{i_6} - \omega)$ . Then,

$$\chi_\Lambda(I_1, I_2, I_3, J) = +\chi_\omega(a_1, a_2, a_3)\chi(i_0, i_7, i_8, i_9)$$

where  $\chi_\Lambda, \chi$  and  $\chi_\omega$  are the chirotopes of the rank 4 matroids  $M_{\text{Wedge}}(\text{in}(X))$  and  $M_{\text{Lin}}(\text{in}(X)) = M_{\text{Aff}}(X)$  and the rank 3 matroid  $M_{\text{Wit}_\omega}(X)$  respectively.

*Proof.* We shall follow similar arguments as those in the rank 3 case, but this time we need to handle linear and affine issues at the same time. Let  $\alpha_{s_1} = \alpha(I_1)$ ,  $\alpha_{s_2} = \alpha(I_2)$  and  $\alpha_{s_3} = \alpha(I_3)$ .

By Lemma 1, we have

$$(5) \quad \chi_\Lambda(I_1, I_2, I_3, J) = \Delta(x_{i_7}, x_{i_8}, x_{i_9}, \alpha(\alpha_{s_1}, \alpha_{s_2}, \alpha_{s_3})) = -\Delta(\alpha(\alpha_{s_1}, \alpha_{s_2}, \alpha_{s_3}), x_{i_7}, x_{i_8}, x_{i_9}).$$

We shall show that

$$(6) \quad \begin{aligned} \alpha(\alpha_{s_1}, \alpha_{s_2}, \alpha_{s_3}) &= -\chi_\omega(a_1, a_2, a_3)\omega \\ &= -\Delta((x_{i_1} - \omega) \wedge (x_{i_2} - \omega), (x_{i_3} - \omega) \wedge (x_{i_4} - \omega), (x_{i_5} - \omega) \wedge (x_{i_6} - \omega))\omega. \end{aligned}$$

The desired equality follows by combining (5) and (6).

Since  $\alpha_{s_1}, \alpha_{s_2}$  and  $\alpha_{s_3}$  contain the common point  $\omega$  then  $\alpha(s_1, s_2, s_3)$  must be either  $\omega$  or  $-\omega$  (or trivial). We have that

$$\text{sign}(\langle \alpha(s_1, s_2, s_3), \omega \rangle) = \Delta(\alpha_{s_1}, \alpha_{s_2}, \alpha_{s_3}, \omega).$$

We show that

$$(7) \quad \Delta(\alpha_{s_1}, \alpha_{s_2}, \alpha_{s_3}, \omega) = -\chi_\omega(a_1, a_2, a_3).$$

If  $\alpha_{s_k} = \mathbf{0}$  for some  $1 \leq k \leq 3$  then both sides of (7) are equal to 0. We thus suppose that  $\alpha_{s_k} \neq 0$ ,  $1 \leq k \leq 3$ . Notice that both sides of Equation (7) are invariant by translations. Therefore, without loss of generality, we assume that  $\omega = 0$ , and hence,  $\omega = \mathbf{e}_1 = (1, 0, 0, 0)$ . In this setting, the  $\alpha_{s_k}$  are orthogonal to  $\mathbf{e}_1$ , we may thus write  $\alpha_{s_k} = (0, \tilde{\alpha}_{s_k})$ . Moreover, by definition, in the corresponding linear space  $\mathbb{R}^4$ ,  $\alpha_{s_1}$  is the vector orthogonal to

$$\left\langle \mathbf{e}_1, \begin{pmatrix} 1 \\ x_{i_1} \end{pmatrix}, \begin{pmatrix} 1 \\ x_{i_2} \end{pmatrix} \right\rangle = \left\langle \mathbf{e}_1, \begin{pmatrix} 0 \\ x_{i_1} \end{pmatrix}, \begin{pmatrix} 0 \\ x_{i_2} \end{pmatrix} \right\rangle,$$

that is,  $\tilde{\alpha}_{s_1}$  is orthogonal to  $\langle x_{i_1}, x_{i_2} \rangle$  and such that

$$\det \begin{pmatrix} 1 & 1 & 1 & 0 \\ 0 & x_{i_1} & x_{i_2} & \tilde{\alpha}_{s_1} \end{pmatrix} = \det \begin{pmatrix} 1 & 0 & 0 & 0 \\ 0 & x_{i_1} & x_{i_2} & \tilde{\alpha}_{s_1} \end{pmatrix} = \det(x_{i_1} \quad x_{i_2} \quad \tilde{\alpha}_{s_1}) > 0.$$

Therefore, we may deduce that  $\tilde{\alpha}_{s_1} = x_{i_1} \wedge x_{i_2} \in \mathbb{R}^3/\mathbb{R}_+$ .

By proceeding with similar arguments, it can be showed that  $\tilde{\alpha}_{s_2} = x_{i_3} \wedge x_{i_4}$  and  $\tilde{\alpha}_{s_3} = x_{i_5} \wedge x_{i_6}$ , see Figure 9. Finally we have that

$$\Delta(\alpha_{s_1}, \alpha_{s_2}, \alpha_{s_3}, \omega) = \Delta \begin{pmatrix} 0 & 0 & 0 & 1 \\ x_{i_1} \wedge x_{i_2} & x_{i_3} \wedge x_{i_4} & x_{i_5} \wedge x_{i_6} & 0 \end{pmatrix} = -\chi_\omega(a_1, a_2, a_3).$$

□

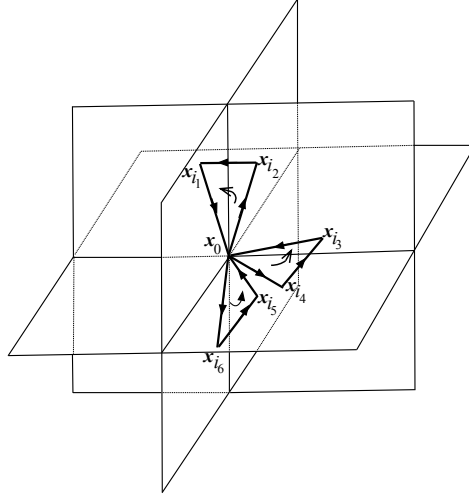


FIGURE 9. This figure sums up the situation of Proposition 2. The three hyperplanes meet positively or negatively at  $x_0$  depending on the sign of the triplet of lines witnessed by  $x_0$ .

#### 4. GEOMETRIC KNOTS

Let us first recall a simple way to encode a knot diagram that enable to reconstruct an equivalent diagram from it.

4.1. **Gauss code.** A *Gauss code* of an oriented knot diagram with  $n$  crossings is constructed as follows. Label all the crossings of the diagram from 1 to  $n$  (in an arbitrary manner). The Gauss code is derived by walking the knot, starting at point  $P$  of the diagram (picked arbitrarily and other than a crossing). As we follow the diagram, we record the crossings we encounter, by writing down the labels preceded with an ‘O’ or ‘U’ to indicate whether the curve goes *Over* or *Under* strand, see Figure 10.

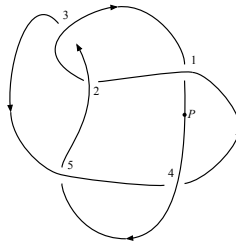


FIGURE 10. Knot  $5_2$  with Gauss code O4 U5 O2 U3 O5 U4 O1 U2 O3 U1.

In general, the Gauss code for a knot diagram cannot be used to reconstruct an equivalent diagram, but an extension of it will make the reconstruction possible. The *extended Gauss code* is a minor revision of Gauss code : as we encounter a given crossing, we recorded it as above and we also assign a sign depending on the handedness of the crossing. If it is *right-handed*, we assign positive; if it is *left-handed*, negative, see Figure 11.

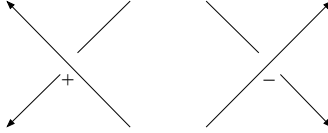


FIGURE 11. Positive and negative oriented crossings.

The extended Gauss code of the example illustrated in Figure 10 is given by

$$O_+4 \ U_+5 \ O_+2 \ U_+3 \ O_+5 \ U_+4 \ O_-1 \ U_+2 \ O_+3 \ U_-1.$$

A diagrammatic representation of an extended Gauss code is given by a *Gauss diagram* constructed as follows. Take an oriented circle with a base point chosen on the circle. Walk along the circle marking it with the labels for the crossings in the order of the Gauss code. Now draw chords between the points on the circle that have the same label. Orient each chord from the over crossing to the under crossing in the Gauss code. Mark each chord with + or - according to the sign of the corresponding crossing in the Gauss code. An example of the Gauss diagram for the knot  $6_3$  is given in Figure 12.

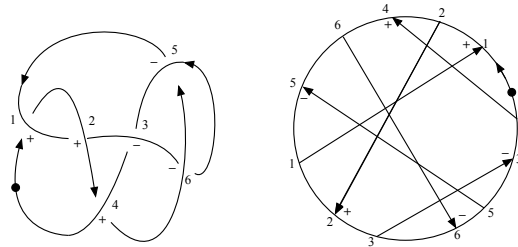


FIGURE 12. (Left)  $6_3$  with Gauss code  $U_+1 \ O_+2 \ U_+4 \ O_-6 \ U_-5 \ O_+1 \ U_+2 \ O_-3 \ U_-6 \ O_-5 \ U_-3 \ O_+4$  (Right) Corresponding Gauss diagram.

It is known that a knot diagram on the sphere can be recovered uniquely (up to isotopy) from its Gauss diagram which can thus be considered as an alternative way to present knots. Unfortunately, not every picture which looks like a Gauss diagram is indeed a Gauss diagram of some knot. This is not easy to recognize, see [2].

A Gauss diagram can also be represented by an oriented line where the ends are identified and having oriented signed arcs corresponding to the chords, see in Figure 13.

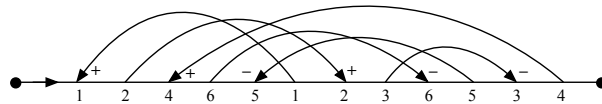


FIGURE 13. Line representation of the Gauss diagram illustrated in Figure 12.

**4.2. Main result.** Let  $y_0 \in \mathbb{R}^3$  and let  $\pi_{y_0}$  be the radial projection emitting from  $y_0$  to  $\mathbb{S}^2$ , that is,

$$\begin{aligned} \pi_{y_0} : \mathbb{R}^3 \setminus \{y_0\} &\rightarrow \mathbb{S}^2 \\ y &\mapsto \frac{y-y_0}{\|y-y_0\|} \end{aligned}$$

Let  $K$  be a knot in  $\mathbb{R}^3$ . We may associate to  $K$  a *sphere shadow* which is just the radial projection  $\pi_{y_0}(K)$ . We may suppose that such a shadow is regular in the sense that it avoids cusps and tangency

points (this can be obtained by making some suitable local modifications to  $K$  without changing its type). Let  $z$  be a point in  $\pi_{y_0}(K)$ , suppose that

$$z = \pi_{y_0}(y_1) = \dots = \pi_{y_0}(y_k), \quad k \geq 1$$

where  $\|y_1\| < \dots < \|y_k\|$  with  $y_1$  is the nearest to  $y_0$ .

We say that  $z$  is a *simple intersection* if  $k = 2$  and a *multiple intersection* if  $k \geq 3$ . We may also avoid multiple intersections  $z$  by moving pieces of the shadow around  $z$  properly. To this end, it is enough to consider  $k - 2$  concentric circles  $C_k, \dots, C_2$  of radius  $\epsilon_{k-2} > \dots > \epsilon_2$  all of center  $z$  and move the piece of arc  $i = k, \dots, 2$  inside  $C_i$  to its boundary. Notice that these modifications do not change the type of  $K$  and they are done orderly from the furthest to the nearest point to  $y_0$ , see Figure 14. We notice that these local diagrams arising on this way only depends on the order in which the different strands met as we turn around the intersection point.

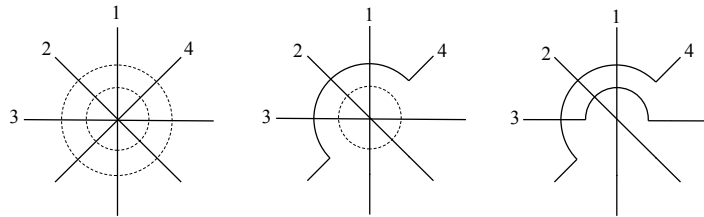


FIGURE 14. Sequence of modifications done around a multiple intersection.

Therefore, sphere shadows can be thought of as a 4-regular map (i.e., an embedding of a 4-regular planar graph into  $\mathbb{S}^2$ ). An *spherical diagram* of  $K$  is obtained from such a shadow by endowing the under/over information to each vertex, see Figure 15.

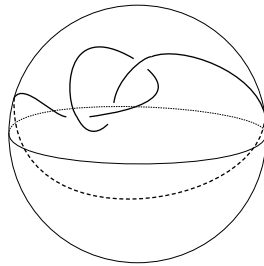


FIGURE 15. A spherical diagram of the Trefoil.

A spherical diagram is still a knot diagram of  $K$  in the usual sense. In particular, knots having isotopic spherical diagrams are isotopic.

We may now prove Theorem 1.

*Proof of Theorem 1.* Let  $X = \{x_0, \dots, x_{n-1}\}$  be a set of points in  $\mathbb{R}^3$  in general position. Let  $K$  be the polygonal knot formed by segments  $[x_0, x_1] \cup [x_1, x_2] \cup \dots \cup [x_{n-1}, x_0]$ . We show that  $\text{SGeom}(M(X))$  determines uniquely the type of  $K$ . Let us consider the radial projection  $\pi_{x_0}$  emitting from  $x_0$  of  $K$ . Notice that the semi-open intervals  $(x_0, x_1]$  and  $(x_0, x_{n-1}]$  are each mapped into a single point. Since  $K$  is polygonal then  $\pi_K$  may have tangency point that can be fixed as described above, see Figure 16.

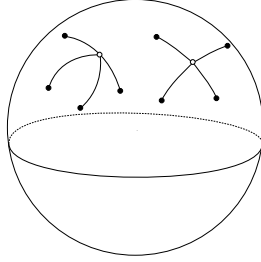


FIGURE 16. Possible tangencies (white circle) appearing in the projection  $\pi_{x_0}(K)$ . (Left) Tangency of an arc and ends of two arcs (Right) tangency of two ends of arc.

The shadow  $\pi_{x_0}(K)$  may also have multiple points  $z$  that can be modified as described above. We can keep record of where (and the order) of the new intersections are done if the the order of the points  $y_i$  (with respect to the distance to  $y_0$ ) having  $\pi_{x_0}(y_i) = z$  as image is known.

This radial projection does not arise a spherical diagram but rather a *spherical line* diagram, that is, an embedding of a planar graph with all the vertices having degree 4 except for two special ones of degree one, see Figure 17.

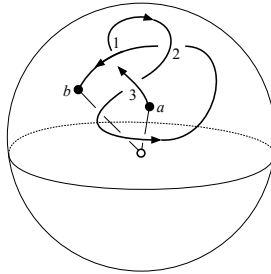


FIGURE 17. A spherical line diagram of a *line eight-figure* knot.

We may associate a Gauss *path diagram* to a spherical line diagram in a similar manner as a Gauss diagram is associated to a knot diagram. Take an oriented segment, say  $S$ , with an initial and end points. Walk along  $S$  marking it with the labels for the crossings in the order they are encountered. Now draw arcs between the marks on  $S$  that have the same label. Orient each arc from the over crossing to the under crossing in the spherical line diagram. Mark each arc with + or - according to handedness' rule, see Figure 18.

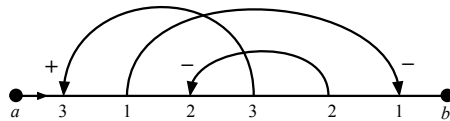


FIGURE 18. The Gauss path diagram arising from the spherical line diagram given in Figure 17.

**Claim 1.** *If two polygonal knots have the same Gauss path diagram then they are isotopic.*

*Proof.* We will show that Gauss path diagram determines the spherical line diagram (up to a planar isotopy). This might be done by slightly adapting the classic procedure to show that Gauss diagrams determine knot diagrams given in [6]. However, here we propose a new different approach. We shall

see that any face of the spherical line diagram can be determined by using the Gauss path diagram. We shall show that the set of faces (and whether two of them share an edge) in the spherical line diagram correspond to a set of *valid* travels in the Gauss path diagram.

Let us consider a walk  $W$  on the arcs on the boundary of a face (say, anticlockwise) in the spherical line diagram. Notice that we can run through an arc either following its direction or in opposite direction, see Figure 19.

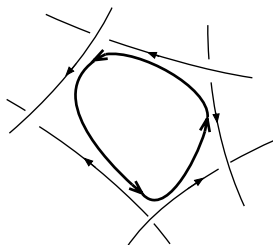


FIGURE 19. Walk around a boundary of a face.

We associate to  $W$  a travel  $T$  along the Gauss path diagram. Turns of  $W$  at a crossing correspond to jumps in arrows (from head/tail to tail/head) and each arc in  $W$  corresponds to a piece of the oriented segment  $S$  (of the Gauss path diagram). Travel  $T$  may follow or not the direction of  $S$  (depending on whether or not  $W$  follows the direction of the corresponding arc). Since  $W$  goes around a face then this correspondence obeys certain rules according to the sign of the crossing and from which strand (over/under) the walk comes from and goes to. These rules are illustrated in Figure 20.

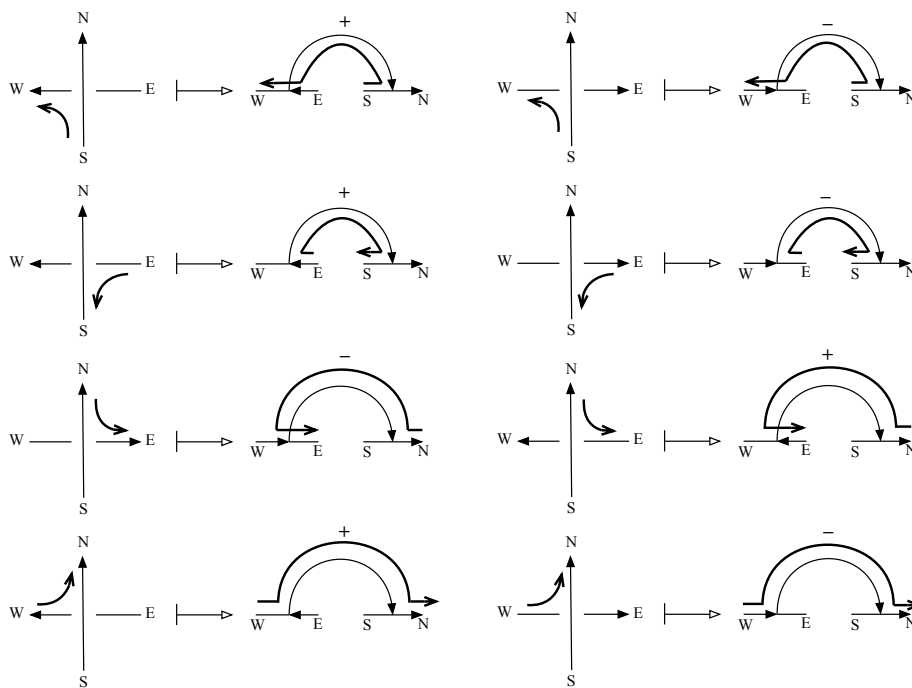


FIGURE 20. Local turnings of a walk around a crossing and the corresponding local travel in the Gauss path diagram (in bold).



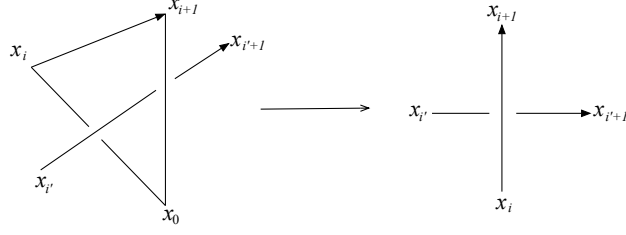


FIGURE 23. Radon partition and crossing from the witness.

Furthermore, if  $\pi_{x_0}([x_i, x_{i+1}])$  and  $\pi_{x_0}([x_{i'}, x_{i'+1}])$  intersect, the oriented arcs (from  $x_i$  to  $x_{i+1}$  and from  $x_{i'}$  to  $x_{i'+1}$ ) on the sphere meet at a positive crossing if and only if  $\chi(x_i, x_{i+1}, x_0, x_{i'+1}) = +1$ . For a multiple intersection, the Radon partition determine which arc is above/below the others. We can thus record the order of the new intersections (and on which arc) after the local modifications explained above.

For (B), we notice that the rotation order of several strands around a multiple point only depends on the set of signs of the pairs of crossings which can be determined by the same argument as in (A).

For (C), suppose that both arcs  $\beta' = \pi_{x_0}([x_{i'}, x_{i'+1}])$  and  $\beta'' = \pi_{x_0}([x_{i''}, x_{i''+1}])$  intersect arc  $\beta = \pi_{x_0}([x_i, x_{i+1}])$ . The order of the intersection, say from  $\pi_{x_0}(x_i)$  to  $\pi_{x_0}(x_{i+1})$  is given by the chirotope  $\chi_{x_0}$  according with the rule given in Figure 24. We notice that, by Proposition 2,  $\chi_{x_0}$  can be completely determined from  $\chi$  and  $\chi_\Lambda$ .

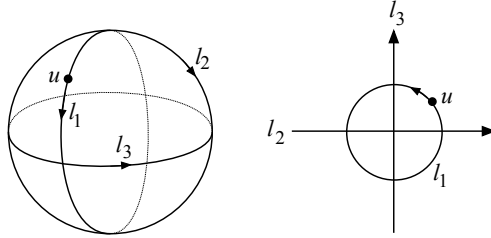


FIGURE 24. If  $\chi_{x_0}(1, 2, 3) = +1$  then, by walking along  $l_1$  following its direction, say from  $u$ ,  $l_1$  meets  $l_3$  negatively, then  $l_2$  positively, then  $l_3$  positively and finally  $l_2$  negatively.

Let  $l_1 = i \wedge (i + 1)$ ,  $l_2 = i' \wedge (i' + 1)$  and  $l_3 = i'' \wedge (i'' + 1)$ . Then, by following Figure 24 with  $\chi_{x_0}(1, 2, 3) = +1$  we have that

$$\text{if } \beta \text{ crosses } \begin{cases} \beta' \text{ positively and } \beta'' \text{ positively then } \beta \text{ meets } \beta'' \text{ before } \beta', \\ \beta' \text{ positively and } \beta'' \text{ negatively then } \beta \text{ meets } \beta' \text{ before } \beta'', \\ \beta' \text{ negatively and } \beta'' \text{ negatively then } \beta \text{ meets } \beta'' \text{ before } \beta', \\ \beta' \text{ negatively and } \beta'' \text{ positively then } \beta \text{ meets } \beta' \text{ before } \beta''. \end{cases}$$

The result follows. □

## 5. FURTHER RESEARCH DIRECTIONS

In the process of this work, a great deal on the structure, properties and extensions of the notion of strong geometry have been revealed.

Ringel’s isotopy conjecture asked whether any two arrangements of lines with the same topological type can be isotoped into each other. In other words, Ringel’s conjecture asked whether the realization space of rank 3 matroids is connected. The famous Mnëv Universality Theorem [8] provides a spectacular negative solution, it states that every semi-algebraic variety is stably equivalent to the realization space of some oriented matroid, that is, the realization space of oriented matroids can have the topology of any semi-algebraic set and, in particular, it can be disconnected. As mentioned above, oriented matroids do not capture the combinatorics of the cell configuration induced by the spanned lines contrary to strong geometries that completely does. In the same flavor as for oriented matroids, we investigate [5] a universality result à la Mnëv for rank 3 strong geometries.

The spherical line diagrams were introduced to deal with the fact that the radial projection is from a point belonging to the polygonal knot. This might be avoided if given two set of points  $P$  and  $Q$  having the same strong geometry then one can show the existence of two points  $p$  and  $q$  such that  $P \cup \{p\}$  and  $Q \cup \{q\}$  also have the same strong geometry. In this case, we just can add this additional point from which the radial projection is applied. Figure out the existence of these new points is not difficult when  $d = 2$  but it is not straightforward for  $d \geq 3$ .

It turns out that the notion of strong geometry can be generalized in the planar case as follows. We consider the lines spanned by both the set of the original points and the points arising from line intersections. The latter induce a new set of lines and therefore new intersection points from which new lines can be spanned and so on. These generalizations happen to be closely related to the notion of  $k$ -equivalence between two configurations of points (the case  $k = 1$  concerns the existence of a new point to be added to a strong geometry, as discussed above). A notion of  $\infty$ -equivalence also naturally emanate.

Finally, as pointed in the proof of Claim 1, we introduce a new way to show that a knot diagram can be determined by the corresponding Gauss diagram. We believe that this approach can be extended to investigate *spatial graphs* and *virtual knots*.

All these investigations require further (much technical) extra work (in progress).

#### REFERENCES

- [1] A. Björner, M. Las Vergnas, B. Sturmfels, N. White and G. Ziegler, Oriented Matroids, *Encyclopedia of Mathematics and its Applications* **46** Cambridge University Press (1999).
- [2] G. Cairns and D.M. Elton, The planarity problem for signed Gauss words, *J. Knot Theory and Its Ramifications* **2** (1993) 359-367.
- [3] J. Chappelon, L. Martínez-Sandoval, L. Montejano, L.P. Montejano, J.L. Ramírez Alfonsín, Codimension two and three Kneser transversals, *SIAM J. Discrete Mathematics*, **32** (2018), 1351–1363.
- [4] J.E. Goodman and R. Pollack, Multidimensional sorting, *SIAM J. Computing* **12** (1983), 484—507.
- [5] B. Gros and J.L. Ramírez Alfonsín, Strong geometry II : universality, in preparation.
- [6] L.H. Kauffman, Virtual knot theory, *Europ. J. Comb.* **20** (1999), 663–691.
- [7] M. Las Vergnas, Personal communication (1995).
- [8] N.E. Mnëv, The universality theorem on the oriented matroid stratification of the space of real matrices, *In Discrete and Computational Geometry : Papers from the DIMACS Special Year (1990)*, J. E. Goodman, R. Pollack, and W. Steiger, Eds., vol. 6 of DIMACS Series in Discrete Mathematics and Theoretical Computer Science, DIMACS/AMS, pp. 237–244.

IMAG, UNIV. MONTPELLIER, CNRS, MONTPELLIER, FRANCE  
*Email address:* `baptiste.gros@umontpellier.fr`

IMAG, UNIV. MONTPELLIER, CNRS, MONTPELLIER, FRANCE  
*Email address:* `jorge.ramirez-alfonsin@umontpellier.fr`